A DRIVER-HETEROGENEOUS CAR-FOLLOWING MODEL

José Muñoz-Figueroa, Universidad de Chile, jomunozf@gmail.com
Cristián E. Cortés, Universidad de Chile, ccortes@ing.uchile.cl
Francisco Martínez Concha, Universidad de Chile, fmartine@ing.uchile.cl

ABSTRACT

We extend and merge Mahut's and Newell's car-following models to include heterogeneous desired speeds of vehicles, which becomes relevant for proper mimicking of platoon formation and evolution. The proposed model offers a complete description of traffic dynamics over a given highway stretch, where delays occur at the end. Illustrative numerical examples are conducted with several model specifications, showing scattering of the fundamental diagrams, the "capacitydrop" phenomena, and stop-and-go waves related to "phantom jams"; therefore it shows traffic hysteresis as well.

Keywords: car-following model, driver heterogeneity, traffic dynamics

1 INTRODUCTION

Vehicular traffic problems have been widely studied in several contexts for decades; researchers have devoted important resources in order to have a more comprehensive understanding of vehicular traffic phenomena, as these problems have grown rapidly in many places around the world. In an effort to study control strategies for traffic congestion, and to optimize traffic control more effectively in situations of high stress of the system, traffic simulation at different scales has been the most utilized tool as through this technique it is possible to dynamically reflect the characteristics of vehicle traffic flow. A relevant module of most simulation schemes at a microscopic (vehicle) level is the car-following model, based on the idea that each driver controls a vehicle, responding to the stimuli from the preceding vehicle.

Car-following models have a long history in transport, with more than 60 years of scientific research, and their main premise is to try to mimic the particularities of vehicle movement across roads; with the outstanding enhancement in computation power of the last decades, these models have become essential part of most micro-simulation commercial packages, which are used in transportation planning and evaluation in many cities and countries around the world (Barceló, 2010). Moreover, they are a key part of the design of intelligent transportation systems (ITS), and naturally can be used for developing collision-warning and collision-avoidance (CW & CA) systems (Brackstone & McDonald, 2000; Li & Sun, 2012). Obviously, further understanding of car-following models becomes more and more important as advanced technologies develop.

In practically all car-following model specifications and frameworks proposed so far, the outputs are speeds or accelerations of vehicles across (discretized) time. Thus, integration is needed to determine the spatiotemporal trajectories of vehicles (e.g. for fundamental diagram analysis), or the travel times across a given road length[1]. One remarkable exception is the car-following model proposed by Mahut (1999, 2000), conceived from the idea of safe-stopping distances, whose output are directly the time-space trajectories of vehicles; moreover, analytical travel time functions can be determined for a given road length with delays at the end of the segment, feature that improves computation times in networks as simulation along arcs over time is not required. This model assumes identical vehicles in three parameters: desired speed, effective vehicle length, and response time.

Independently, Newell (2002) states a car-following model based on spatiotemporal trajectories analysis with linear spacing (depending on the platoon speed), whose propagation formula can be seen as an extension of Mahut's one in order to include heterogeneous space and time displacements (or headways) across vehicles (effective vehicle length and response time in Mahut's context); Daganzo (2006) provides a discrete-time scheme to calculate the spatiotemporal trajectories, and Laval & Leclerc (2010) enhances these formulae in a case of time-varying space and time headways (and bounded acceleration), to mimic what authors called "timid" or "aggressive" behavior, definitions aimed by empirical analysis . Subsequent empirical studies with this model (e.g. Chen et al., 2012) suggest that the time-varying nature of time and space headways triggers traffic hysteresis (Laval, 2011).

[1] This is especially relevant for micro-simulation packages, in terms of computation times and resources for simulating transportation networks.

In this work, we extend and merge Mahut's and Newell's car-following models in order to include heterogeneous desired speeds of vehicles; this possibility was discussed informally by Newell (2002) in several paragraphs of his paper, highlighting the relevance of desired speeds' variability in platoon formation and evolution. The proposed model offers a complete description of traffic dynamics over a given highway segment where, in addition, delays occur at the end of such stretch (as done by Mahut, 2000). Notice that the conceptual basis of our proposed model generates two independent traffic congestion sources: the propagation of disturbances, and the asymmetric effect of speed differences along the road.

The structure of the paper is as follows. In Section 2 we summarize the related literature considered fundamental for building our extended model, highlighting the details of the seminal works for our proposal. In Section 3 we present all the details of our model, treating separately each interesting case. In Section 4 we validate our model through illustrative simulation experiments, to finally in Section 5 make all relevant analysis and conclusions together with proposed further work in several interesting related research lines.

2 RELATED WORK

In Newell's car-following model (Newell, 2002), if the nth vehicle is following the $(n-1)$th vehicle by time t, then the space-time trajectory of the nth vehicle at t, $x_n(t)$, will be a translation, in both space and time, of the space-time trajectory of the $(n-1)$th vehicle at time t, $x_{n-1}(t)$, that is to say,

$$x_n(t) = x_n(t - \tau_n) - d_n \tag{1}$$

The translation parameters $\tau_n \wedge d_n$ in (1) are the space headway and the time headway of the nth vehicle respectively, and therefore this model assumes a linear relationship between preferred spacing s_n and the speed v of the lead vehicle, given by

$$s_n(v) = d_n + \tau_n v \quad \forall n, \text{ with } v \in [0, V_n]$$

where V_n is the "desired-speed" of the nth vehicle; this last parameter was highlighted by Newell (2002) as one of the determinants in the circulation speed of vehicles forming a platoon. In fact, the author states textually "… Each driver would also have some *desired speed* V_n and if the $(n-1)$th vehicle should travel with $v > V_n$, the nth would travel at the velocity V_n … , and the two vehicles would separate". Moreover, regarding the speed of a platoon, namely v, he states: "… The value of v could be the V_k for some vehicle downstream $k < n$". It is worth mentioning that Newell (2002) ends his article with the following sentence: "…To apply the theory one must specify what happens at some points downstream presumably at some inhomogeneity in the highway…If the present model is correct, future attention can be focused on where and why flow changes originate."; as the formula (1) is valid only under congested conditions, this model only explains how disturbances propagate downstream in a platoon of vehicles.

Daganzo (2006) provides a time-discrete version of Newell car-following model (2002), given by

$$x_n^i = \min\{x_n^{i-1} + \tau v_f, x_{n-1}^{i-1} - \lambda\} \tag{2}$$

where i is the ith time-step, v_f is the (common) free-flow speed, τ is the duration of the time-step (and the time headway), and λ is the minimum possible spacing; the time-continuous version of (2) is given by (Laval & Leclercq, 2010)

$$x_n(t) = \min\{x_n(t-\epsilon) + \epsilon v_f, x_{n-1}(t-\tau) - \lambda\} \tag{3}$$

In the case of homogeneous vehicles (i.e. $\tau_n = \tau, d_n = \lambda, V_n = v_f \; \forall n$), there is a recognized connection between Newell's car-following model and the kinematic wave model based on a triangular fundamental-diagram with jam density $\kappa = 1/\lambda$, free flow speed v_f, and wave speed $\omega = -\lambda/\tau$; in fact, equation (3) is the exact mathematical solution of such a model (Laval & Leclercq, 2010). Although this last equation is valid for almost any $t \geq \epsilon > 0$, in the literature it is common to set $\epsilon = \tau$. Later on, and motivated from empirical analysis of real-life vehicle streams, Laval and Leclerc (2010) extends (3) in order to mimic what authors called *timid* or *aggressive* driver behavior, in terms of deviations from its exact "Newell trajectory"; this was conducted by including a dimensionless term $\eta_n(t)$ multiplying both space and time headways in (3), yielding the following specification

$$x_n(t) = \min\{x_n(t-\epsilon) + \min\{\epsilon v_f, \tilde{x}_n(t)\}, x_{n-1}(t - \eta_n(t)\tau) - \eta_n(t)\lambda\} \tag{4}$$

The first term of (4) slightly differs from the first term of (3) as this model also includes bounded-acceleration of vehicles, while the second term refers to the follower' behavior with time-variable headways; timid driver behavior exists when $\eta_n(t) > 1$, whereas aggressive behavior takes place with $\eta_n(t) < 1$. In Chen *et al.* (2012), this model was validated using empirical trajectory data from NGSIM (Next Generation SIMulation, 2010), unveiling that driver heterogeneity (in terms of *timid* or *aggressive* behavior) can explain the spontaneous formation and ensuing propagation of stop-and-go waves in congested traffic.

It is worth mentioning that the works of Mahut (1999, 2000) - who started from safe stopping distance rules - obtained the same trajectory-relationship (1) as that of Newell under congested regime[2] for homogeneous vehicles; furthermore, he actually solved the model for a given stream of vehicles traveling across a one-lane highway of length $X = K\lambda$ for some $K \in \mathbb{N}$ (this is done in order to discretize space), with two special points: an origin, and an end. In the former, a demand process that determines the *effective departure times* of vehicles is stated; for the latter, a (exogenous) delay process is considered for every vehicle; in the sense of Newell (2002), these are two basic inhomogeneities of a highway that permits to state a complete modeling framework. In addition, Mahut's solutions were obtained in terms of time-space trajectories $t_n(x)$, which can be conceived as the inverse of the spatiotemporal trajectories, obtained by simply rotating the $x - t$ plane where the trajectories are, in 90º counterclockwise; one of the main advantages of working with these trajectories is that initial conditions are naturally related to the demand times; in contrast, in spatiotemporal trajectories the time dimension is measured from the perspective of the nth driver, which precludes the correct interpretation of the term $x_{n-1}(t - \tau_n)$, and makes difficult the statement of initial conditions $x_n(0)$. Although this can be overcome by re-defining the $x_n(t)$'s to a universal time measure, in time-space trajectories the

[2] This means that the Newell's car-following model is collision-free.

space measure is naturally universal, as the highway length to be covered is the same for everyone. The author provides two specifications of the model: a cell-based approach and an arc-based approach. In the former, space is discretized (with step size of λ) in order to simulate traffic dynamics; in the latter, the computation of travel times does not require the simulation of trajectories over the arc length, feature that considerably improves the performance in computation resources compared with other well-known car-following models (e.g. Nagel & Schreckenberg, 1992).

In the present paper, first we obtain a continuous-space version of Newell's propagation formula for the time-space trajectories $t_n(x)$, including vehicles with heterogeneous desired speeds, in addition to different space and time headways as well. Then, we solve this extended model in a Mahut-like context, that is to say, we assume a one-lane highway with two special points, origin and end. In the former, an *effective departure time* process takes place in order to assure the minimum spacing requirements (as the model is collision-free); for the latter, a delay is assigned to every outgoing vehicle before actually exiting the highway, which can propagate downstream if some conditions hold (roughly speaking, if the following stream of vehicles are close enough each other).

3 METHODOLOGY

As a general framework, we consider a set of N drivers, and for each driver i we include three parameters: the space headway d_i, the time headway τ_i, and the desired speed u_i. In addition, we consider a one-lane highway of length L, containing two special points: the origin, and the end of the stretch. Next in section 3.1, we characterize the behavior at these relevant two points.

Additionally, in all subsequent analysis, we assume that the time-space trajectories are the "*càdlàg*" inverse of the spatiotemporal trajectories, in the sense that for every n^{th} vehicle, any period of time in which the speed becomes equal to zero at a generic spatial-point x, say ω_n^x, will be captured by the time-space trajectories in the following way

$$t_n(x) \equiv t_n(x^-) + \omega_n^x, \text{ where } t_n(x^-) = \lim_{\delta \to 0^+} t_n(x-\delta) \tag{5}$$

that is to say, in the spatial-point x the function $t_n(x)$ has a horizontal jump of length ω_n^x. As we will see next, the end of the highway will be, in principle, the only point in space in which (5) is stated as we impose delays right there.

3.1. Inhomogeneities of the highway

3.1.1 The origin of the highway

We assume in the origin that every driver i is endowed with a preferred time $\mathfrak{t}_i \geq 0$ to enter the highway; this instant is commonly referred in the literature as the "preferred" *departure time,* or the *demand time* of such a driver. Now, for any given vector of demand times $\mathfrak{t}$, there is a re-labeling σ that sort drivers from early to late demand times; for the remainder of this work, it is assumed that $\mathfrak{t}$ (and therefore σ) are known and fixed. In order to make the formulae derived hereafter more readable, we recognize $\sigma(n)$ as the nth driver; this maintains the classical convention used in a car-following context.

When complete heterogeneous vehicles are included (i.e. different desired speeds and headways), it is straightforward that equation (3) can be generalized to this setting by simply replacing v_f by the desired speed of the nth driver u_n, τ by the driver-specific time headway τ_n, and λ by d_n, that is to say

$$x_n(t) = \min\{x_n(t-\epsilon) + \epsilon u_n, x_{n-1}(t-\tau_n) - d_n\} \tag{6}$$

Complementarily, from the definition of the time-space trajectories we have the following identity

$$x_n\big(t_n(x)\big) \equiv x \ \forall n, \text{ in almost every point}^3 \ x \tag{7}$$

This last identity permits to "invert" (6) on time, in order to obtain a specification for the time-space trajectories $t_n(x)$. In fact, if we evaluate (6) at $t = t_n(x)$, we have

$$\begin{gathered} x \equiv x_n\big(t_n(x)\big) = \min\{x_n(t_n(x)-\epsilon) + \epsilon u_n, x_{n-1}(t_n(x)-\tau_n) - d_n\} \\ \Rightarrow \\ x_n(t_n(x)-\epsilon) \leq x - \epsilon u_n \ \wedge \ x_{n-1}(t_n(x)-\tau_n) \leq x + d_n \end{gathered} \tag{8}$$

Now, using (7), we have that

$$x - \epsilon u_n \equiv x_n\big(t_n(x-\epsilon u_n)\big) \ \wedge \ x + d_n \equiv x_{n-1}\big(t_{n-1}(x + d_n)\big)$$

In addition, the spatiotemporal trajectories are monotone and non-decreasing (as negative speeds are not allowed). Combining these two facts into (8) gives the following inequalities for $t_n(x)$

$$\begin{aligned} &\text{(a)} \quad t_n(x) \geq t_n(x-\delta) + \frac{\delta}{u_n} \\ &\text{(b)} \quad t_n(x) \geq t_{n-1}(x + d_n) + \tau_n \end{aligned} \tag{9}$$

where $\delta = \epsilon u_n$. These inequalities can be combined in a single formula, which is

$$t_n(x) \geq \max\left\{t_n(x-\delta) + \frac{\delta}{u_n}, t_{n-1}(x + d_n) + \tau_n\right\} \tag{10}$$

The final assumption is that drivers attempt to reach the distance x, starting from $x - \delta$, at their minimum time[4], which allow us to state equation (10) as an equality; that is to say

$$t_n(x) = \max\left\{t_n(x-\delta) + \frac{\delta}{u_n}, t_{n-1}(x + d_n) + \tau_n\right\} \tag{11}$$

[3] The points in which this is not true are the so-called *braking* points.
[4] This assumption is the same used by Daganzo (2005) for the derivation of formula (2).

We impose that the initial conditions for (11) are precisely the (preferred) departure times, i.e.

$$t_n(0) = \mathbb{t}_n \ \forall n \tag{12}$$

It is interesting to see what happens when (11) is evaluated at $x = \delta$, and (12) is used; this leads to

$$t_n(\delta) = \max\left\{\mathbb{t}_n + \frac{\delta}{u_n}, t_{n-1}(\delta + d_n) + \tau_n\right\}$$

By taking the limit $\delta \to 0^+$, we obtain the following relationship

$$t_n(0^+) \equiv \lim_{\delta \to 0^+} t_n(\delta) = \max\{\mathbb{t}_n, t_{n-1}(d_n) + \tau_n\} \tag{13}$$

The limit[5] $t_n(0^+)$ is defined as the *effective* departure time of the nth vehicle, and correspond to the earliest feasible time instant in which the vehicle can actually depart from the origin (instead of the preferred departure time) due to the presence of the preceding vehicle on the road.

3.1.2. The end of the highway

Equation (11) permits the computation of time-space trajectories for a given distance x_0; it is easy to see that for the nth driver, the relevant value of the time-space trajectory for the $(n-1)$th driver corresponds to the time needed to reach distance $x_0 + d_n$, and for this driver the relevant value of the time-space trajectory for the $(n-2)$th driver corresponds to distance $x_0 + d_n + d_{n-1}$, and so on; in all these steps, we are assuming that preceding vehicles are still on the road.

What happens at the end of the highway is that drivers experience delays before they can actually exit from it; this means that vehicles spend positive time intervals at the same place, which are precisely the cases in which the spatiotemporal trajectories cannot be inverted in the sense of (7); in this case, we use the expression in (5) in order to compute the value of the time-space trajectory for distance L, that is to say, $t_n(L) \equiv t_n(L^-) + \omega_n \ \forall n$, recalling that $t_n(L^-)$ is conceptually the instant in time when the nth vehicle reaches the end of the highway. Moreover, we impose that when the $(n-1)$th vehicle finally exits, at time instant $t_{n-1}(L)$, its influence (in terms of the following process) over the nth vehicle ends; this clearly has an impact in the behavior of the latter vehicle up to this point, and therefore on the value of $t_n(L^-)$.

To illustrate what happens, let us think that the nth vehicle were actually following the $(n-1)$th vehicle by time instant $t_{n-1}(L)$ when this vehicle finally exits the highway segment; this disturbance, that we call the *vanishing* of the $(n-1)$th vehicle, is realized by the nth driver at time $t_{n-1}(L) + \tau_n$. If we evaluate (1) with $t = t_{n-1}(L) + \tau_n$ we will obtain

$$x_n(t_{n-1}(L) + \tau_n) = x_{n-1}(t_{n-1}(L) + \tau_n - \tau_n) - d_n \equiv L - d_n$$

[5] The limit has the expression $\max\{\mathbb{t}_n, t_{n-1}(d_n) + \tau_n\}$ because $\mathbb{t}_n + \frac{\delta}{u_n}$ is a linear function.

Then, by the time the nth driver realizes that the $(n-1)$th vanishes, there is still a distance d_n to be covered for reaching the end of the highway. As there are no other obstacles within the nth vehicle and the end, this distance d_n is traveled at the desired speed u_n; then, the time instant $t_{n-1}(L)+\tau_n+\frac{d_n}{u_n}$ captures the precise moment for the nth driver to reach the end of the highway, and therefore the following lower bound for $t_n(L)$ can be determined

$$t_n(L) \geq t_{n-1}(L)+\tau_n+\frac{d_n}{u_n}+\omega_n$$

In general, as the time-space trajectories are non-decreasing, we can state the following identity, for a given $0<\delta<L$: $t_n(L^-) \geq t_n(L-\delta)+\frac{\delta}{u_n}$. This is true as when the nth driver is at distance $L-\delta$ by time $t_n(L-\delta)$, the end of the highway can be reached in a time instant at least equal to $t_n(L-\delta)+\frac{\delta}{u_n}$; besides, the limit when $\delta \to 0^+$ of the right side equals $t_n(L^-)$. Then, we can bound $t_n(L)$ from below by

$$t_n(L) \geq t_n(L-\delta)+\frac{\delta}{u_n}+\omega_n$$

The combination of the previous lower bounds for $t_n(L)$ yields

$$t_n(L) \geq \max\left\{t_n(L-\delta)+\frac{\delta}{u_n}, t_{n-1}(L)+\tau_n+\frac{d_n}{u_n}\right\}+\omega_n$$

At this point, we assume that drivers attempt to exit the highway in the minimum possible time, which is equivalent to state the last inequality as a equality. All the previous analysis analysis allow us to state the following system of equations for the endpoint of the highway

$$\begin{gathered} t_1(L)=t_1(L-\delta)+\frac{\delta}{u_1}+\omega_1 \\ t_n(L)=\max\left\{t_n(L-\delta)+\frac{\delta}{u_n}, t_{n-1}(L)+\tau_n+\frac{d_n}{u_n}\right\}+\omega_n \end{gathered} \tag{14}$$

Equations (11), (12) and (14) can be discretized simply by considering x to be an entire multiple of δ, as well as L and the space headways d_n; this discretization scheme is presented in section 4, in order to conduct simulations.

4. SIMULATIONS AND DISCUSSION

In this section we will show through numerical examples the impact of our modeling approach on capturing the fact of observing heterogeneous drivers, agglomeration due to depart time choices, and propagation of delays downstream on highway traffic; the impact is measured by comparing our framework with a lead vehicle problem (LVP), a Mahut-delay instance (MD), and the combined instance of the previous two[6], under two scenarios with full-heterogeneous drivers: deterministic and stochastic driver behavior. In the former, the car-following parameters d_n, τ_n and u_n are fixed across simulations; for the latter, we allow these parameters to vary within each simulation step. In order to simulate the time-space trajectories generated by our proposed model, we discretized space in steps of a given length $\delta > 0$; the space-discrete traffic dynamics for the stream of vehicles (except the first) comes from (11) and (14), with x to be an integer multiple of δ, as well as the space headways d_i and the highway length, i.e. $d_i = r_i\delta \, , r_i \in \mathbb{N} \ \forall i$ and $L = M\delta$. In fact, taking $x = k\delta$ in (14) and $L = M\delta$ in (17) yields

$$t_n^k = \begin{cases} \max\left\{t_n^{k-1} + \frac{\delta}{u_n}, t_{n-1}^{k+r_n} + \tau_n\right\} & if \ k + r_n \leq M \\ t_n^{k-1} + \frac{\delta}{u_n} & if \ k + r_n > M \wedge k < M \\ \max\left\{t_n^{M-1} + \frac{\delta}{u_n}, t_{n-1}^{M} + \tau_n + \frac{r_n\delta}{u_n}\right\} + \omega_n & if \ k = M \end{cases} \tag{15}$$

where $t_n^k \equiv t_n(k\delta) \ \forall k, n$. In (15), it is understood that $t_n^0 = \mathbb{t}_n \ \forall n$, i.e. the initial conditions are the preferred departure times, which come from sampling *iid* uniform distributions with support on the interval $[\mathbb{t}_{\min}, \mathbb{t}_{\max}]$. In order to provide a complete picture of the traffic dynamics generated by the model, we include three possible instances:

1. A lead vehicle problem (LVP), which consists in assuming a given discrete-space trajectory $\{t_1^k : k = 0, \ldots, M\}$ for the first driver, and with no delays at the end, i.e. $\omega_n = 0 \ \forall n$ in (15).
2. The Mahut-delay instance (MD), that is to say, a free-flow behavior for the first driver (i.e. $t_1^k = t_1^{k-1} + \frac{\delta}{u_1} \ \forall k < M$), with delays ω at the end for all vehicles[7].
3. The combined LVP+MD instance, which is simply the LVP problem considered in point 1, in addition with the delays at the end given in point 2.

It is worth mentioning that specification 3 uses the same LVP trajectory of specification 1 and the same delays of specification 2 in order to construct an adequate benchmark when comparing the different specifications. The LVP trajectory for specifications 1 and 3 is obtained first by sampling circulation speeds u_1^k for every space-step k using a (continuous) uniform distribution on the interval $[u_0, \frac{u_{\min}+u_{\max}}{2}]$, where u_0 is a "minimum-circulation" speed, and then assuming a (random) given subset $Brk \subset \{2, \ldots, M-1\}$ of *braking points*, and a braking time τ^0; with these ingredients, the LVP trajectory[8] is constructed as follows

$$\text{If } k \notin Brk, \text{ then } t_1^k = t_1^{k-1} + \delta/u_1^k \text{ ; if not, } t_1^k = t_1^{k-1} + \tau^0$$

For specifications 2 and 3, the delays at the end of the stretch are sampled from an uniform distribution over the interval $[\omega_{\min}, \omega_{\max}]$.

6 This instance encompasses a lead vehicle problem, with delays at the end.

7 For the first driver, this means that $t_1^M = t_1^{M-1} + \frac{\delta}{u_1} + \omega_1$

8 In specification 3, the last term of the LVP trajectory changes slighty to $t_1^M = t_1^{M-1} + \delta/u_1^M + \omega_1$

The (integer) space-headway r_n for the nth driver is sampled from a (discrete) uniform distribution over the range $\{r_{\min}, r_{\max}\}$, the time-headway τ_n comes from sampling a (continuous) uniform distribution with support on the interval $[\tau_{\min}, \tau_{\max}]$, and the desired speed u_n is given by an uniform random variable over the interval $[u_{\min}, u_{\max}]$; we assume that all these random variables are independent and identically distributed. The parameters of the simulations are showed in Table 1, next.

Table 1. Parameter values for simulations

Parameter	Value	Units	Parameter	Value	Units
N	100	Vehicles	$\mathfrak{t}_{\min}$	1	Hours (from zero)
δ	0.01	Kilometers	$\mathfrak{t}_{\max}$	3	Hours (from zero)
M	1500	-	$\tau_{\min}$	10	Seconds
$\omega_{\min}$	20	Seconds	$\tau_{\max}$	30	Seconds
$\omega_{\max}$	40	Seconds	$u_{\min}$	40	Kilometers/Hour
$r_{\min}$	4	-	$u_{\max}$	120	Kilometers/Hour
$r_{\max}$	10	-	u_0	1/4	Kilometers/Hour
Δx	0.4	Kilometers	Δt	0.2	Hours
τ^0	0.04	Hours	K	5000	-

The parameters Δx and Δt are related to the calculations of fundamental-diagrams using Edie's method (Edie, 1965) over the time-space trajectories; more precisely, Δx and Δt are the spatial and temporal size of the window used to calculate the aggregate measures of flow, density and speed; in these calculations, a random set of K rectangular windows in the $x - t$ plane are generated randomly.

4.1. Scenario A: deterministic driver behavior.

In this scenario, the simulated time-space trajectories are shown at Figure 1

Figure 1. space-time trajectories for scenario A

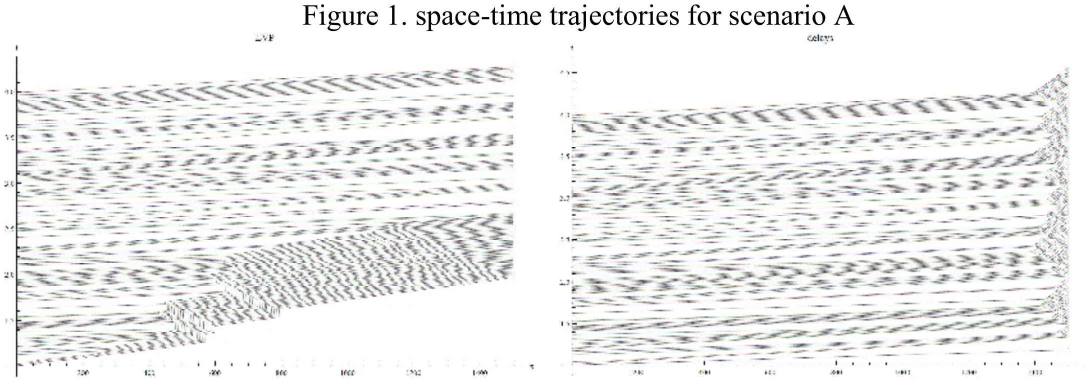

(a) Trajectories for the LVP instance *(b) Trajectories for the MD instance*

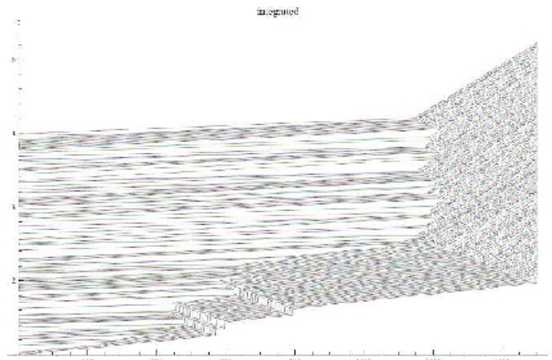

(c) Trajectories under the integrated instance

First of all, it is clear the effect of different desired speeds in platoon formation, merging and diverging across the road in these graphs. In fact, under the MD instance, we can clearly see how these different desired speeds have a significant impact on the magnitude of delays propagation; under this setting, there are more propagation of delays due to platoon rising and merging across the highway segment. As expected, disturbances propagates as a random-walk, because the headways parameters varies across drivers. The associated fundamental diagrams are presented in Figure 2 next.

Figure 2. Fundamental-diagrams for scenario A.

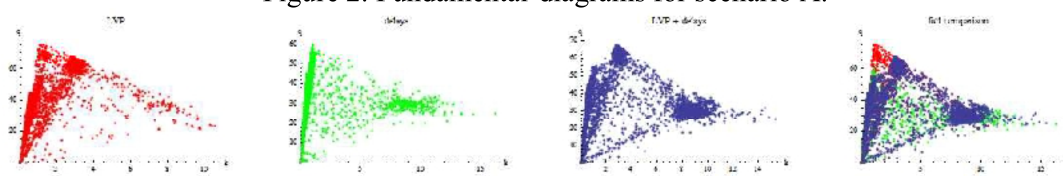

(a) flux vs density diagrams

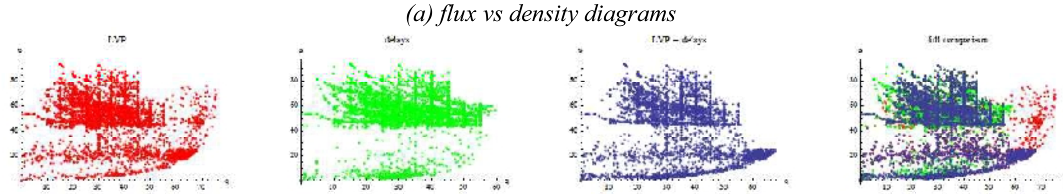

(b) speed vs flux diagrams

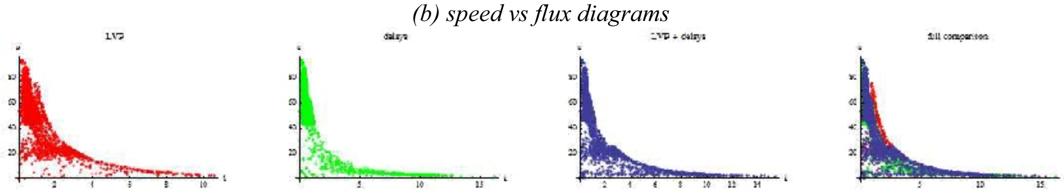

(c) speed vs density diagrams

Now, for the flux-density diagrams, there is a major impact in the non-congested branch; when different speeds are considered, the uncongested branch of the diagram becomes a highly dense cloud of points; in fact, it is easy to realize that this cloud is constrained inside a cone (i.e. an area between two straight lines), with boundaries given by the free-flow diagrams $q = ku$ of the fastest and the slowest vehicle respectively, and the mentioned cone is the area between these segments. Inside this cone we found all (k, q) points calculated using a time-space window that captures only propagation of speed differences. Therefore, the classical assumption of a single straight line for the non-congested branch can be inadequate when full heterogeneity of vehicles is considered, and the extent of this bias is related to the range of fluctuation of the desired speeds. It is worth mentioning that hysteresis is not present in this model by construction, as drivers on a platoon comply with (1) at all times; therefore, the acceleration and deceleration paths becomes the same. Besides, it is known that Newell's car-following model (Newell, 2002) does not reproduce hysteresis; Laval (2011) and Ahn *et al.* (2013) argued that hysteresis is more related to timid or aggressive driver behavior (in terms of deviations from "Newell trajectories"), which can be added to the framework by letting d_i and τ_i to vary with time. We address this issue in the next scenario, where we allow the model parameters to vary between simulation steps, as developed in Section 4.2 next.

4.2. Scenario B: stochastic driver behavior

In this scenario, we allow the vehicle's parameters r_n, τ_n and u_n to vary between simulation steps; the space-discrete scheme for this case becomes

$$t_n^k = \begin{cases} \max\left\{t_n^{k-1} + \dfrac{\delta}{u_n^k}, t_{n-1}^{k+r_n^k} + \tau_n^k\right\} & if\ k + r_n^k \leq M \\ t_n^{k-1} + \dfrac{\delta}{u_n^k} & if\ k + r_n^k > M \wedge k < M \\ \max\left\{t_n^{M-1} + \dfrac{\delta}{u_n^k}, t_{n-1}^M + \tau_n^k + \dfrac{r_n^k \delta}{u_n^k}\right\} + \omega_n & if\ k = M \end{cases}$$

where r_n^k, τ_n^k and u_n^k are the nth vehicle's parameters at step k. The r_n^k's are sampled using a discrete uniform distribution over the range $\{r_n - \Delta r, r_n + \Delta r\}$, with Δr being a natural number such as $r_n - \Delta r \geq 1\ \forall n$; in the simulations performed it was chosen $\Delta r = 3$. For the τ_n^k's, a continuous triangular distribution is used over the interval $[\tau_{\min}, \tau_{\max}]$, with maximum probability at τ_n. Finally, the speed u_n^k is taken equal to $u_n^k = u_n + u^k$, where u^k is drawn from an uniform distribution over the interval $[-\Delta u, \Delta u]$, for a given value of Δu; in simulations, $\Delta u = 30$ was considered. The simulated trajectories are shown at Figure 3.

Figure 3. . space-time trajectories for scenario B

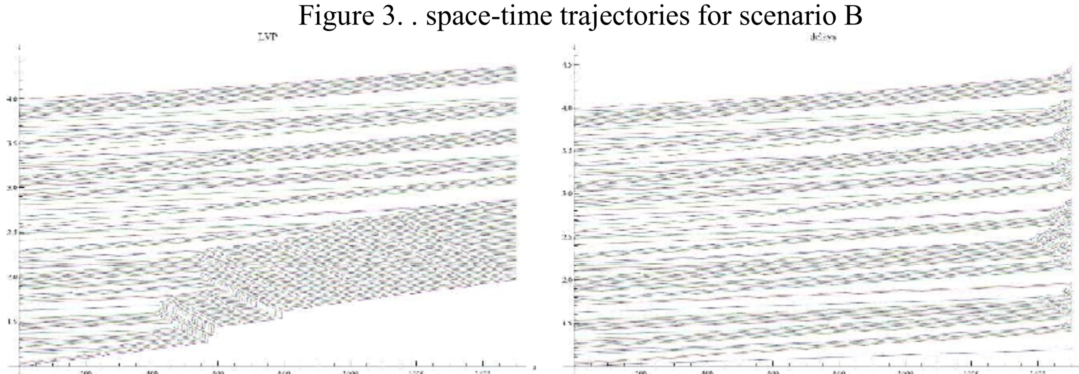

(a) Trajectories for the LVP instance *(b) Trajectories for the MD instance*

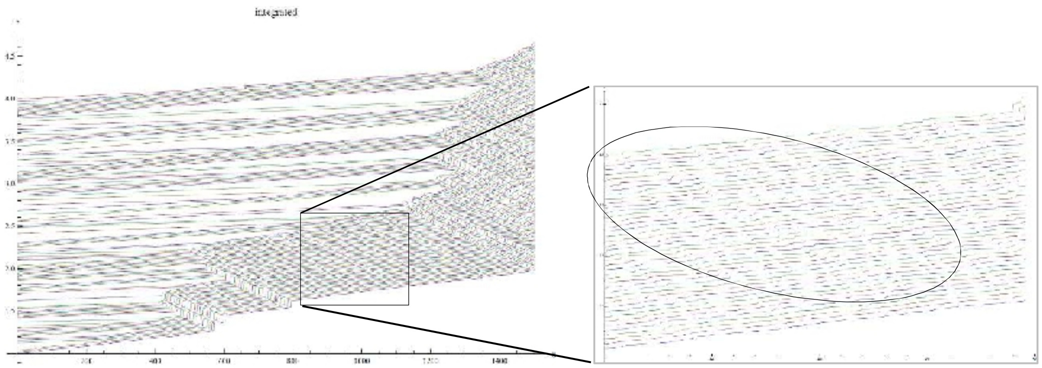

(c) Trajectories under the integrated instance

As expected, the simulated trajectories exhibit "phantom jams" (some of them highlighted in Figure 3.c in the zoom area); they appears due to the same reasons stated by Laval (2011) and Ahn *et al.* (2013), that is to say, by the deviations of the vehicle headway's parameters across time. Moreover, as the headways are varying constantly, the propagation path also changes constantly, even for the same set of vehicles, and therefore delays or another disturbances can either expand or contract, depending of the behavior of the vehicles forming the platoon at that specific point in time, and then, it is expected this model to generate hysteresis as well, as it is very similar to the model developed by Laval and Leclerc (2010) where hysteresis loops are shown.

The fundamental diagrams for this case are the following

Figure 4. Fundamental-diagrams for scenario B

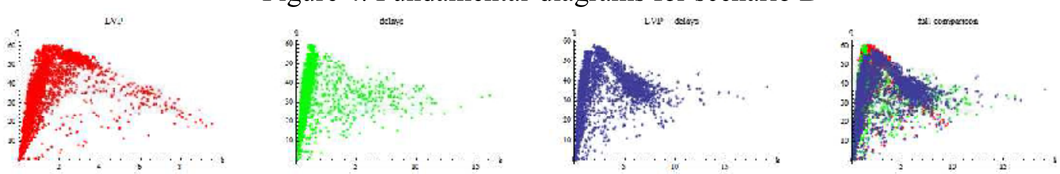

(a) flux vs density diagrams

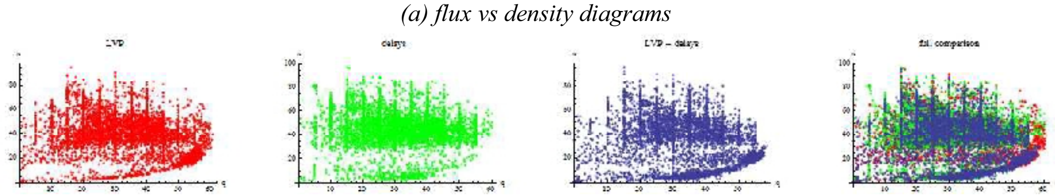

(b) speed vs flux diagrams

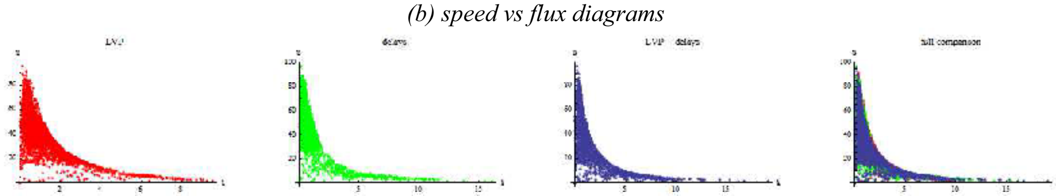

(c) speed vs density diagrams

In the same line of reasoning of previous scenarios findings, the LVP instance still reaches high-flux states due to the discharging of the platoon caused by the first vehicle; most surprising, the other instances reach higher flux-states, compared with previous scenarios: one explanation of this could be the randomness induced by step-varying headways and speeds, which precludes reaching these high states, where all vehicles behave in a deterministic way.

5. Synthesis and conclusions

We extend Mahut's and Newell's car-following models in order to include vehicles with different desired speeds. The model establishes a comprehensive description of traffic dynamics over a given highway segment, with delays occurring at the end. Illustrative numerical examples of time-space trajectories and fundamental diagrams derived from such trajectories were presented in the last section, showing that the proposed model exhibits the "capacity-drop" phenomena, as well as wide scattering in all fundamental diagrams.

Besides, congestion generated by speed differences is clearly observable from the trajectories in Figure 1, showing the effect of considering full heterogeneity in vehicle streams. In addition, a stochastic version was also simulated, showing the presence of phantom jams and stop-and-go waves, related to the hysteresis phenomenon.

This model completes the story started by Newell: the congestions arise because of heterogeneity of desired speeds, agglomeration due to departure time choices, and downstream propagation of delays at the end of the highway. This model generates platoons even in the absence of delays, and also predicts merging and diverging of platoons across time and space, triggered by speed differences as well as the (downstream) propagation of disturbances.

Acknowledgments
We acknowledge the support of FONDECYT grant 1100239; the Risk Habitat Megacities project funded by Hemlholtz Society, Germany; Conicyt's grant that J Muñoz's PhD studies; Instituto de Sistemas Complejos de Ingeniería (ICM: P-05- 004-F, CONICYT: FBO16).

References

Ahn, S., Cassidy, M., and Laval, J. (2004) Verification of a simple car-following theory. **Transportation Research B**, 38, 431-440.

Ahn, S., Vadlamani, S., and Laval, J. (2013) A method to account for non-steady state conditions in measuring traffic hysteresis. **Transportation Research C,** 34, 138-147.

Barceló, J. (2010) **Fundamentals of Traffic-Simulation**. Springer.

Brackstone, M., and McDonald, M. (1999) Car-following: a historical review. **Transportation Research F**, 2, 181-196.

Chen, D., Laval, J., Zheng, Z., and Anh, S. (2012) A behavioral car-following model that captures traffic oscillations. **Transportation Research B**, 46, 744-761.

Daganzo, C.F. (2006) In traffic flow, cellular automata = kinematic waves, **Transportation Research B**, 29, 277-286.

Edie, L.C. (1965) Discussion of traffic stream measurements and definitions. **In: 2nd Int. Symp. on Transportation and Traffic Theory**, Paris, France, 139–154.

Laval, J.A., and Leclercq, L., (2010) A mechanism to describe the formation and propagation of stop-and-go waves in congested freeway traffic. **Philosophical Transactions of the Royal Society A,** 368, 4519–4541.

Laval, J.A. (2011) Hysteresis in traffic flow revisited: An improved measurement method. **Transportation Research B**, 45, 385-391.

Li, Y., and Sun, D. (2012) Microscopic car-following model for the traffic flow: the state of the art. **Journal of Control Theory and Applications**, 10, 133-143.

Mahut, M. (1999) Speed-maximizing car-following models based on safe stopping rules. **Transportation Research Board, 78th Annual Meeting**, January 10-14, Washington DC, US.

Mahut, M. (2000) From Traffic Flow To Queueing Theory. **81th Annual Meeting of Euro Working Group on Transportation**, September 1 1- 14, Rome, Italy.

Nagel, K., and Schreckenberg, M., (1992) A cellular automaton model for freeway traffic. **Journal de Physique I**, 2, 2221–2229.

Newell, G. F. (2002) A simplified car-following theory: a lower order model. **Transportation Research B**, 40, 396-403.

NGSIM (2010) **Next Generation Simulation**. <http://ngsim-community.org/>.